Photochemical Isomerization of Colchicine and Thiocolchicine

ARTICLE *in* THE JOURNAL OF PHYSICAL CHEMISTRY A · OCTOBER 2003

Impact Factor: 2.69 · DOI: 10.1021/jp035507l

Photochemical Isomerization of Colchicine and Thiocolchicine

Laura Bussotti,[†] Ivo Cacelli,[‡] Maurizio D'Auria,*[,§] Paolo Foggi,[||] Giordano Lesma,[⊥] Alessandra Silvani,[⊥] and Vincenzo Villani[§]

LENS, Università di Firenze, Via N. Carrara 1, 50019 Sesto Fiorentino, Firenze, Italy, Dipartimento di Chimica e Chimica Industriale, Università di Pisa, Via Risorgimento 35, 56126 Pisa, Italy, Dipartimento di Chimica, Università della Basilicata, Via N. Sauro 85, 85100 Potenza, Italy, Dipartimento di Chimica, Università di Perugia, via Elce di sotto 8, 06123 Perugia, Italy, and Dipartimento di Chimica Organica e Industriale, Università di Milano, Via Venezian 21, 20133 Milano, Italy

Received: May 30, 2003; In Final Form: August 22, 2003

The photochemical reactivity of colchicine and thiocolchicine is described. Although the irradiation of colchicine gave a well-known transposition reaction to β- and γ-lumicolchicines, thiocolchicine did not react. Femtosecond transient spectroscopy of colchicine showed a strong band with maximum at 510 nm appearing at $\tau = 0$. It disappeared within few hundred femtoseconds, leaving a broad structureless band with a maximum around 470 nm. A second band is observed around 410 nm. The analysis in time showed that the 510-nm component appeared instantaneously and decayed following a biexponential low with time constants of 300 ± 100 fs and 40 ps. The kinetics at 420 nm has a measurable rise time of 300 ± 150 fs. Quantum mechanical calculations on colchicine showed that this absorption is due to a $S_1 \rightarrow S_{11}$ transition. In thiocolchicine, the instantaneous formation of a structure with maxima out of the investigated spectral region was observed. A strong absorption around 650 nm indicated the presence of a band with a maximum at longer wavelengths (> 700 nm) and a peak around 380 nm, which partially coincides with the ground-state absorption and therefore strongly affected by its bleaching. The instantaneous formation of an absorption around 650 nm and its rapid (∼500 fs) decay was observed. At shorter wavelengths (400 nm), the decay was fitted with a biexponential curve with the first time constant of about 80 ps. The second part of the decay had a very long tail up to 500 ps. Transient spectroscopy and configuration interaction calculations are in agreement with a mechanism involving a disrotatory cyclization of colchicine in its first excited singlet state. The lack of reactivity observed in thiocolchicine was explained by considering the presence of efficient ISC to the triplet state.

Colchicine (**1**) is the major alkaloid of *Colchicum autumnale* (autumn crocus) and *Gloriosa superba* (flory lily), Liliacee. It is an ancient drug used in medicine for its antimitotic, antiinflammatory, and antineoplastic effects.[1,2] It has been used as a neurotoxin in animal models of Alzheimer's disease and epilepsy.[3] Several derivatives have been synthesized in order to improve antitumor activity.[4−6]

The irradiation of colchicine leads to the formation of β- and γ-lumicolchicine (**3** and **4**) (Scheme 1). Prolonged irradiation times lead to the formation of α-lumicolchicone (**2**) (Scheme 1).[7−21] β-Lumicolchicine is a biologically active compound.[22]

Previous photolysis studies indicated that the quantum yield of colchicine conversion depends on solvent polarity.[23] This behavior was explained by assuming the formation of a solvation complex in the ground state. The nature of the excited state responsible for the formation of photoproducts has not been determined; the authors proposed that colchicine isomerization occurs from the triplet excited state. However, in a subsequent study, they did not observe any quenching effect of several triplet acceptors on the reactivity.[24] In a previous paper, we found that transient absorption spectroscopy of colchicone and

SCHEME 1: Photoisomerization of Colchicine

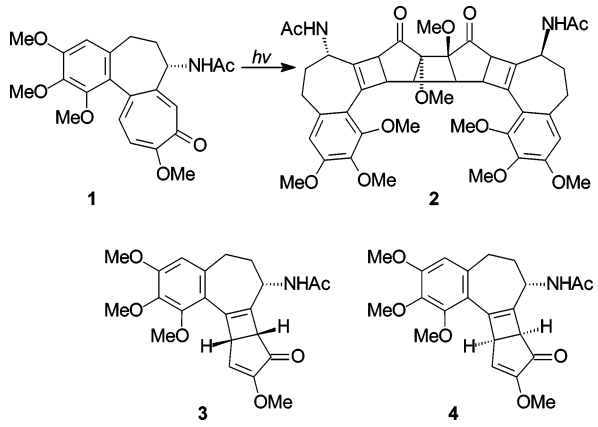

β-lumicolchicone indicated that photoisomerization occurred on colchicone in its first excited singlet state.[25] Furthermore, another study argued against the intermediacy of a colchicine triplet state in the photoisomerization and stressed the role of specific solvent−solute interaction in determining the partitioning of the excited singlet state into β- and γ-lumicolchicine formation.[26] However, in this case, the authors do not draw any definitive conclusions about the nature of the excited states involved in the reaction.

In this work, we report a novel study of the photochemical and photophysical behavior of colchicine (**1**) and thiocolchicine

* Corresponding author. E-mail: dauria@pzuniv.unibas.it. Tel: +39 0971 202240. Fax: +39 0971 202223.
[†] LENS.
[‡] Università di Pisa.
[§] Università della Basilicata.
[||] Università di Perugia.
[⊥] Università di Milano.

10.1021/jp035507l CCC: $25.00
Published on Web 10/03/2003

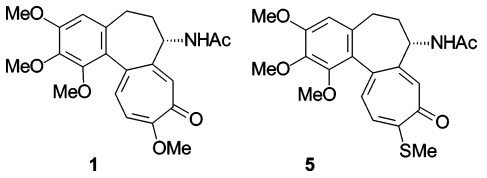

Figure 1. Colchicine (**1**) and thiocolchicine (**5**).

(**5**) (Figure 1). Our data fit the hypothesis that photoisomerization occurs from the first singlet excited state. DFT and extended multireference configuration interaction calculations are carried out to reinforce such a hypothesis.

Materials and Methods

Colchicine (1). The dark-brown gum (330 g) from the alcohol extract of *Colchicum* seeds is diluted with 540 mL of water, and the solution, which contains undissolved solid and resinous material, is heated with 75 g of paraffin wax until the wax is molten. The mixture is stirred vigorously and then allowed to cool. The solid wax, which dissolves the resin, is lifted from the surface, and the process is repeated twice with fresh wax. The combined wax layers are extracted three times with 100 mL of boiling water, and the aqueous extracts are added to the solution of the alkaloid. A paste of filter paper pulp (50 g) (prepared by boiling filter paper with concentrated hydrochloric acid to effect complete disintegration; the mass is then washed with water until neutral) is then added to the aqueous colchicine solution. The mixture is filtered on a filter bed, to which some paper pulp has already been added, and yields a clear brown solution. The filter bed is boiled with a little water and then refiltered. The combined filtrates are extracted with 12 200-mL portions of chloroform, with care being taken to ensure that the chloroform is free from hydrochloric acid. The addition of potassium carbonate to the yellow extract causes the precipitation of some brown flocculent material, which is filtered from the dried solution. The latter is evaporated, leaving a golden-brown syrup. The syrup is redissolved in chloroform (150 mL), and the solution is passed through a column of alumina, previously saturated with benzene. Three bands are formed—an upper, reddish-brown band; a larger, bright-yellow band; and a lower, almost colorless band that contains colchicine. The column is washed with chloroform until the yellowish eluate becomes colorless and yields no residue on evaporation. The distillation of chloroform out of the total eluate gives a golden-yellow syrup, which is distilled three times with an equal volume of absolute alcohol to remove the residual chloroform. The residue is finally crystallized from ethyl acetate and yields 10 g of colchicine as fine colorless needles, mp 148−150 °C. ^{1}H NMR ($CDCl_3$, δ): 8.62 (1 H, d, $J = 6$ Hz), 7.70 (1 H, s), 7.41 (1 H, d, $J = 11$ Hz), 6.91 (1 H, d, $J = 11$ Hz), 6.54 (1 H, s), 4.68 (1 H, dt, $J_1 = 12$ Hz, $J_2 = 6$ Hz), 4.04 (3 H, s), 3.95 (3 H, s), 3.90 (3 H, s), 3.70 (3 H, s), 2.50 (2 H, m), 2.36 (1 H, m), 2.02 (1 H, m), 1.96 (3 H, s). ^{13}C NMR ($CDCl_3$, δ): 179.0, 170.2, 164.3, 153.2, 152.8, 151.2, 141.3, 136.8, 136.0, 134.4, 130.4, 125.6, 113.4, 107.0, 61.5, 61.3, 56.5, 56.3, 53.2, 36.3, 29.2, 22.4.

Thiocolchicine (5). Colchicine (2.5 g) and PTSA (0.3 g) at −80 °C were treated with cold CH_3SH (15 g) in a sealed tube. The mixture was warmed to −20 °C, and a yellow solution was obtained. The mixture then became red. After several days at −80 °C, CH_3SH was distilled between 20 and 40 °C. The residue was dissolved in a water−EtOAc mixture. The organic phase was treated with $NaHCO_3$ until neutrality was achieved. The evaporation of the solvent gave 2.6 g of a brown gum. After crystallization with 10 mL of EtOAc, 2.1 g (80%) of thiocolchicine was obtained, mp 190 °C. ^{1}H NMR (DMSO-d_6, δ): 8.66 (1 H, d, $J = 7$ Hz), 7.26 (1 H, d, $J = 11$ Hz), 7.12 (1 H, d, $J = 11$ Hz), 7.00 (1 H, s), 6.78 (1 H, s), 4.33 (1 H, m), 3.92 (3 H, s), 3.85 (3 H, s), 3.47 (3 H, s), 2.44 (3 H, s), 2.30 (1 H, m), 2.22 (1 H, m), 2.12 (1 H, m), 1.82 (1 H, m), 1.77 (3 H, s). ^{13}C NMR (DMSO-d_6, δ): 181.0, 168.5, 157.5, 153.4, 151.5, 150.4, 141.0, 137.8, 134.3, 134.0, 128.0, 126.8, 126.0, 107.9, 61.2, 61.0, 55.9, 51.4, 35.5, 29.1, 22.3, 14.4.

Photochemical Reactions. Colchicine and thiocolchicine (10 mg) were dissolved in methanol (10 mL) and irradiated for 1 h with a 125-W high-pressure mercury arc lamp (Helios-Italquartz) surrounded by a Pyrex water jacket. The solvent was evaporated, and the crude product was chromatographed on silica gel. Elution with acetone−CH_2Cl_2 2:8 gave the products. In the case of colchicine, β- and γ-lumicolchicine were obtained. The irradiation of thiocolchicine did not give products. β-Lumicolchicine: ^{1}H NMR ($CDCl_3$, δ): 6.66 (1 H, d, $J = 3$ Hz), 6.50 (1 H, s), 6.20 (1H, d, $J = 7$ Hz), 4.82 (1 H, m), 4.09 (1 H, dd, $J_1 = J_2 = 3$ Hz), 3.96 (3 H, s), 3.90 (3 H, s), 3.85 (3 H, s), 3.70 (3 H, s), 3.60 (1 H, dd, $J_1 = 3$ Hz, $J_2 = 2$ Hz), 2.77 (2 H, dd, $J_1 = 15$ Hz, $J_2 = 9$ Hz), 2.60 (1 H, dd, $J_1 = 15$ Hz, $J_2 = 9$ Hz), 2.04 (3 H, s), 2.00 (1 H, m). ^{13}C NMR ($CDCl_3$, δ): 201.0, 170.1, 158.0, 153.0, 151.5, 145.4, 140.0, 138.5, 128.9, 117.5, 109.2, 61.7, 61.0, 56.8, 56.2, 51.6, 43.3, 32.5, 31.3, 23.5. γ-Lumicolchicine: ^{1}H NMR ($CDCl_3$, δ): 6.65 (1 H, d, $J = 4$ Hz), 6.50 (1 H, s), 6.05 (1H, d, $J = 8$ Hz), 4.64 (1 H, dt, $J_1 = 8$ Hz, $J_2 = 7$ Hz), 4.03 (1 H, dd, $J_1 = 4$ Hz, $J_2 = 3$ Hz), 3.94 (3 H, s), 3.87 (6 H, s), 3.70 (3 H, s), 3.60 (1 H, dd, $J_1 = 3$ Hz, $J_2 = 1$ Hz), 2.66 (2 H, m), 2.00 (3 H, s), 1.96 (2 H, m). ^{13}C NMR ($CDCl_3$, δ): 198.9, 169.3, 157.5, 153.0, 151.5, 146.4, 140.5, 138.9, 138.4, 128.0, 118.0, 109.4, 61.3, 60.8, 56.8, 56.3, 50.4, 43.3, 49.1, 32.3, 30.9, 23.6.

Femtosecond Transient Spectroscopy. The experimental instrumentation and data processing for femtosecond time-resolved transient absorption (TA) spectroscopy have been described in detail in previous papers.[25−29]

Briefly, ultrashort pulses (duration ∼100 fs at 800 nm, repetition rate 1 kHz, energy 700 μJ/pulse) are produced by a Ti:sapphire-based laser system. The output of the amplifier is divided into two portions. The most intense portion generates, through the optical parametric process into a BBO crystal, signal and idler output from 1.2−1.6 and 1.6−2.4 μm, respectively. In the present experiment, the fourth harmonic of the signal (1.38 μm) at 345 nm pumps the colchicine molecules directly into the vibrational manifold of the S_1 state. The weakest portion, 2 μJ/pulse, is focused onto a CaF_2 plate and produces pulses of a slightly chirped white-light continuum.[26−29] A portion of the continuum, from 350 to 700 nm, is selected after reflection onto two broad band dielectric mirrors. The white beam is further split into two parts of equal intensity by a 50/50 fused-silica−Al beam splitter. One of these, acting as the probe beam, spatially overlaps with the excitation beam and measures the transient transmittance at any given delay time. The second interacts with the sample in a different position and provides a convenient reference signal. The intensity is detected by means of a back-illuminated CCD camera with a spectral response in the range of 300−1000 nm. Two horizontal strips covering 350 nm are selected on the CCD target to measure the probe and reference intensities that are spectrally dispersed after passing through a flat-field 25-cm Czerny−Turner spectrograph.

The transient transmittance at a given delay time τ and wavelength λ, $T(\tau, \lambda)$, is defined as $I(\tau, \lambda)/I_0(\lambda)$, where $I(\tau, \lambda)$ and $I_0(\lambda)$ are the intensities of the white-light continuum component at λ reaching the detector having or having not

interacted with the pump pulse, respectively. Two measurements are performed—the first without the pump beam, thus acquiring $I_0(\lambda)$ and $I_R(\lambda)$, and second with both the excitation and probe beams—enabling us to measure $I(\tau, \lambda)$ and $I_R(\lambda)$. The transient transmittance $T(\tau, \lambda)$ is given then by $[I(\tau, \lambda)/I_R(\lambda)]/[I_R(\lambda)/I_0(\lambda)]$, thus removing any fluctuation in the intensity distribution.

Because of the chirping of the white-light continuum, spectral features can appear at different delay times at different wavelengths.[26,29] Transient spectra are therefore corrected according to the procedure described in ref 29. Excited absorption spectra can be modified by the presence of stimulated emission and ground-state bleaching, both leading to positive peaks in the transient transmittance spectra. In the selected spectral range and limited to the blue side (350−400 nm), spectra are affected by ground-state bleaching. The overall effect is that the peaks are red-shifted. This effect must be taken into account when comparing the experimental to the calculated data.

Finally, at very short delays, we also take into account the group velocity mismatch (GVM) that affects the envelope of the cross correlation between the pump and probe pulses.[25,26]

Mathematically, the measured relaxation kinetics are given by the following convolution integral:

$$S(\tau) = \int \mathrm{d}t\, g(t - \tau)\, R(t) \qquad (1)$$

where $S(\tau)$ is the time-dependent signal, $g(t - \tau)$ is the second-order cross correlation between the pump and probe, and $R(t)$ is the molecular response function. Equation 1 is utilized only to extract precise decay constants below 1 ps. Small fluctuations in the pulse duration and energy affect the spectral and temporal characteristics of the white continuum. Therefore, the small daily setup alignments introduce an additional uncertainty in the duration of the instrumental function. This is why we report time constants with errors that are comparable to the duration of the instrumental function. For longer decay times, $g(t)$ can be considered to be a Dirac delta function, and $R(t)$ in practice coincides with $S(\tau)$. In the present case, the main source of error is due to the low intensity of the signals.

To make a more sound comparison between experimental and calculated spectra, we have also evaluated the oscillator strength of the excited-state absorption according to the following procedure.

The excited volume can be approximately described as a cylinder 1.8 mm high with a radius equal to 50 μm. The volume of the cylinder is then $V = 1.4 \times 10^{-5}$ cm^3. The incident UV pulse has a typical energy of 1−2 μJ/pulse. A 345-nm photon has an energy of 5.7×10^{-19} J. In one pulse, there are therefore 1.75×10^{12} photons. Ninety percent of them are absorbed, thus leading to 1.57×10^{12} excited molecules. The concentration of the excited states is therefore 1.8×10^{-4} M.

The transient absorbance is on the order of 0.02, giving a value for ϵ of about 600.

The oscillator strength is given by the following integral:

$$f = 4.33 \times 10^{-9} \int \epsilon(\nu)\, \mathrm{d}\nu \qquad (2)$$

where ν is measured in cm^{-1}.

By a numerical evaluation of eq 2, it is possible to calculate for the entire broad structure shown in Figure 2 an f with a value of approximately 1.2×10^{-2}.

Theoretical Method and Computational Details. The geometry of the ground-state S_0 was optimized both by the Hartree−Fock (HF) method and by density functional theory (DFT) in the B3LYP implementation.[30] For the first singlet excited state S_1, the geometry was optimized at a single-excitation CI (CIS) level in which the active space included the 16 highest occupied orbitals and the 22 lowest empty orbitals. In both cases, the Gaussian 98 package was used.[31] For these calculations, the 6-311G basis with a d polarization function on the C, N, and O atoms was employed. The stability of the results versus the basis set was checked by performing the same calculations with a smaller basis set. It was found that by using the 6-31G basis set the bond distances at the optimized geometries change less than 0.04 Å with respect to those obtained with the larger basis set.

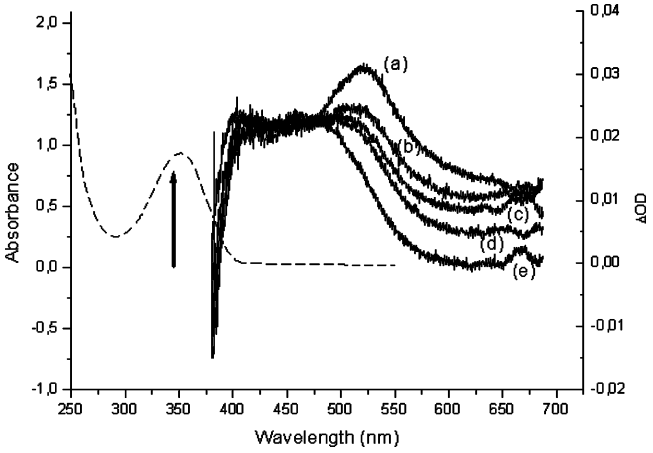

Figure 2. Ground-state absorption (- - -) and TA spectra (—) of colchicine in methanol. TA spectra are recorded at (a) 0.0, (b) 0.3, (c) 0.6, (d) 0.8, and (e) 1.9 ps. The up arrow shows the position of the excitation wavelength. The right scale refers to the ground-state absorbance of a 10^{-3} M solution measured in a 1-cm cell.

For the excitation spectrum, rather extensive configuration interaction (CI) calculations were carried out at the optimized geometries of S_0 and S_1. Both ground and excited states were determined by multireference CI using the CIPSI method[32] in which an initial configurational space, according to the so-called aimed selection,[33] is gradually enlarged by exploiting the first-order perturbative correction of the single and double excitations of this space to the considered eigenstates. The sequence is repeated until a reasonable compromise between the level of accuracy and the computational effort is reached. In the present work, the final configurational space includes about 6000 detors. It must be stressed that the aimed selection can provide a balanced description of the ground and excited states; this is of primary importance when the excitation energies are to be evaluated by the difference in absolute energies. The final variational energies of both the ground and excited states are then corrected by second-order diagrammatic perturbation theory using the Epstein−Nesbet partition scheme.[34] In this step, the contributions of single and double excitations of all Slater determinants belonging to the final configurational space are considered for the energy correction to all N states.

For these calculations, which require the transformation of one- and two-electron integrals from atomic to molecular orbitals, we employed the 6-31G basis set. The effects of the absence of polarization functions on the excitation spectrum were accurately checked by performing calculations of excited states on a smaller system obtained by retaining only the moiety of interest. This will be discussed in the next section.

Results and Discussion

The irradiation of colchicine (**1**) in MeOH for 1 h gave a 1:1 mixture of **3** and **4** (Scheme 2). On the contrary, thiocolchicine did not react (Scheme 2).

SCHEME 2: Photochemical Behavior of Colchicine and Thiocolchicine

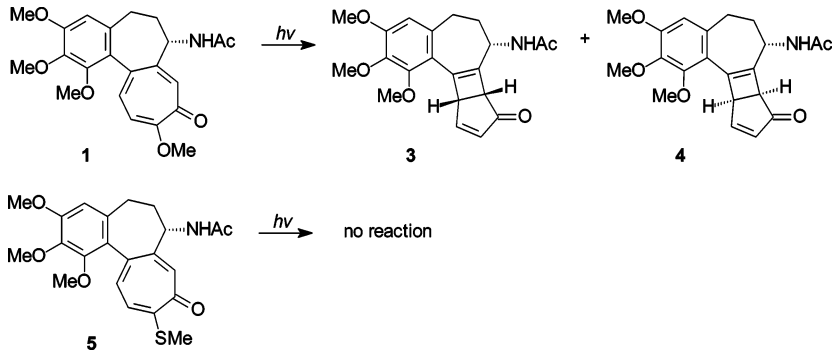

The different behavior of these two compounds moved us to test their photophysical properties. In fact, we have described above that the reaction mechanism of the photochemical transposition of colchicine is not known; furthermore, we do not have a theory that is able to explain the lack of reactivity observed in thiocolchicone

In Figure 2, the excited-state absorption of colchicines is reported as a function of the delay between the pump and probe pulses. A strong band with a maximum at 510 nm (2.43 eV) appears at $\tau = 0$. It disappears within a few hundred femtoseconds, leaving a broad structureless band with a maximum around 470 nm. A second band is observed around 410 nm (3.02 eV). However, it must be considered that in this region ground-state bleaching also occurs (see the stationary absorption of Figure 2), which causes a change in the sign of the ΔOD. This therefore implies that the peak appearing at shorter wavelength is due to the overlapping of two bands adding together with opposite sign. As a consequence, the real maximum occurs at shorter wavelengths than it appears in the spectra. To evaluate its position, we need to know the exact concentrations of excited- and ground-state molecules. We can safely assign this band to a strong transition with a maximum occurring at wavelengths well below 400 nm.

The analysis in time shows different behaviors at different probe wavelengths (Figure 3). The 510-nm component appears instantaneously (within the duration of the cross-correlation function) and decays first with a time constant of 300 $\pm$ 100 fs, followed by a second decay with a time constant of 40 ps. The kinetics at 420 nm has a measurable rise time of 300 $\pm$ 150 fs and the same long decay of 40 ps. This implies that the excitation at 345 nm can populate an excited state that rapidly converts into a second one. Such a rapid process is consistent with a rearrangement of the structure and of the charges after Franck−Condon excitation.

In thiocolchicine, by pumping at 360 nm we observe the instantaneous formation of a structure with maxima out of the investigated spectral region. In fact, a strong absorption around 650 nm indicates the presence of a band with a maximum at longer wavelengths (> 700 nm) and a peak around 380 nm, which partially coincides with the ground-state absorption (Figure 4) and therefore is strongly affected by its bleaching. In the present case, it is very difficult to discuss spectral data and to attribute a particular wavelength to excited-state transitions. However, we were able to measure the dynamical behavior of the signal at different probe wavelengths. What we observed around 650 nm is the instantaneous formation of an absorption and its rapid ($\tau \approx 500$ fs) decay. At shorter wavelengths (400 nm), the signal rise time coincides with the decay of the previous spectral feature, and the decay is fitted with a biexponential curve with the first time constant of about 80 ps. The second part of the decay has a very long tail up to 500 ps.

To explain these experimental results, we performed calculations on colchicine and its excited states. The first calculation is performed at the equilibrium geometry of S_0 in order to study the nature of the first excited states and to compute the absorption spectrum with attention to the intense band experimentally observed around 340 nm (3.65 eV) (Figure 2).

The equilibrium geometry of S_0 determined by the B3LYP/6-311G calculation shows a nearly planar conformation of the

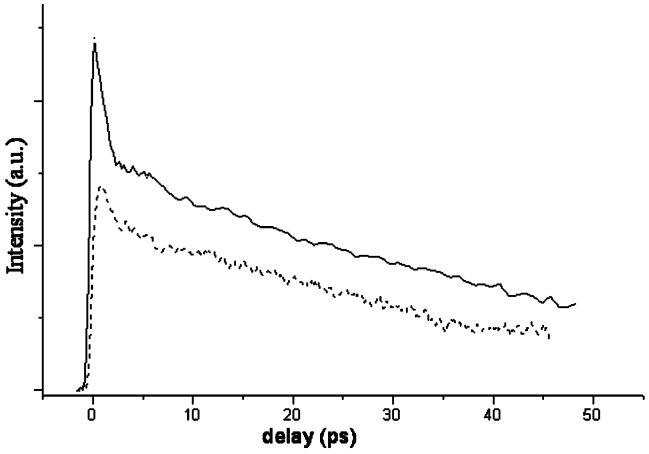

Figure 3. Excited-state absorption of colchicine measured as a function of time at 520 nm (upper trace) and 420 nm (lower trace). The fast decay (300 fs) measured at 520 nm corresponds to the rise time of the signal at 420 nm. The long tail decay is fitted by a biexponential curve with time constants of 40 and 250 fs (see text).

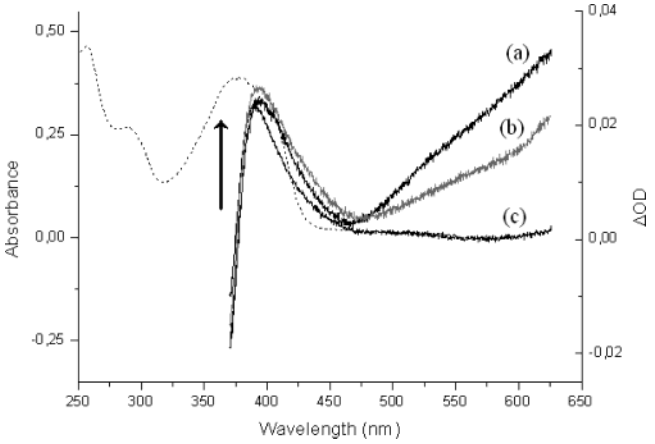

Figure 4. Ground-state absorption (- - -) and TA spectra (—) of tiocolchicine in methanol. TA spectra are recorded at (a) 0.0, (b) 0.5, and (c) 2 ps. After 2 ps, only one band is present around 380 nm. Its position is strongly affected by ground-state bleaching. The up arrow shows the position of the excitation wavelength. The left scale refers to the ground-state absorbance of a 10^{-3} M solution measured in a 2-mm cell.

TABLE 1: Vertical Transition Energies and Oscillator Strengths for the Colchicina Molecule at the Geometry Optimized for the Ground State S_0 Computed by Multireference CI Calculations

state	assignment[a]	ΔE (eV)	f[b]
S_1	$5\pi \rightarrow 6\pi$	5.01	0.20
S_2	$5\pi \rightarrow 7\pi$	5.07	0.24

[a] Excitation label with respect to the main configuration of S_0. The 5π orbital is the HOMO, the 6π is the LUMO, and the 7π is the LUMO+1. All of these orbitals are localized on the tropolone ring. [b] Oscillator strengths calculated in the mixed length−velocity gauge.

seven-atom ring. The deviation from planarity is evaluated by the residues of the involved carbon atoms with respect to their least-squares plane; the maximum value is 0.07 Å. Because even the atoms linked to the carbon atoms of the ring are close to the least-squares plane, it appears that the 2-methoxytropolone moiety is almost planar. The distance between the adjacent carbons belonging to the ring reflects the single- or double-bond nature of the bond: 1.44−1.48 and 1.33−1.35 Å are found, respectively, in the two cases. Because the planes of the two aromatic rings form an angle of 54°, the possibility that the two π clouds strongly interact with each other can be ruled out.

The results of the CI calculation at the equilibrium geometry of S_0, performed with the CIPSI method considering the lowest-three spin-singlet states, are reported in Table 1. From the analysis of the two excited states, it appears that they mainly correspond to single excitations from the highest π orbital (HOMO) to the two lowest unoccupied π^* orbitals, respectively. Because all of these orbitals are localized on the tropolone moiety, a strong f value may be expected. The disagreement between the computed and the experimental transition energies (5 vs 3.65 eV) can be ascribed to the lack of a large part of the electronic correlation energy mainly because the basis set that was used does not include polarization functions.

To demonstrate this assessment, we carried out some calculations on the smaller 2-methoxy-tropolone for which more extended CI calculations with larger basis sets can be performed with reasonable computational effort. The geometry of the reduced system was taken to be equal to that of the colchicine molecule with the two C−C bonds, connecting the tropolone moiety to the rest of the molecule, substituted by C−H bonds. By using the same basis 6-31G and a fraction of the active orbitals larger than that used for the whole molecule, the lowest excitation energies were 4.6 and 4.7 eV. The differences with respect to the 5.01 and 5.07 values reported in Table 1 can be ascribed both to the larger number of active orbitals and to the effects of the surrounding moieties that have been substituted by hydrogen atoms. By using the 6-311G(d) basis set and the same energy window for the active orbitals, we found that the two excitation energies decrease to 3.9 and 4.1 eV, respectively. This net decrease of about 0.6 eV reveals that the correlation energy of S_1 and S_2 is greater than for the ground state, and more reliable excitation energies could be obtained by taking into account a larger fraction of the correlation energy. Of great importance here is the $\pi \rightarrow \pi^*$ nature of the two lowest excited states, which does not change in all of these calculations. Moreover, their small energy difference, which does not change appreciably in these calculations, indicates that the broad observed absorption at 340 nm (3.65 eV) should be ascribed to two overlapping bands corresponding to transitions to S_1 and S_2.

To explain the transient absorption of colchicine, we computed the equilibrium geometry of S_1 and the excitation spectrum at this geometry. In this calculation, we use the CIS method joined with the 6-311G(d) basis set. An analogous calculation of the excitation spectrum of S_2 was not performed because, as will be shown later, the analysis of this state leads us to suppose a low reactivity with respect to S_1. As for S_0, the energy minimum corresponds to a near-planar geometrical arrangement of the tropolone moiety. The bond distances are in general between the typical values corresponding to double and single C−C bonds so that a clear classification of the bond orders is not straightforward in this case. The energy gain of S_1 due to the geometrical relaxation after vertical excitation at the S_0 equilibrium geometry was estimated to be about 0.4 eV. From a classical viewpoint, this can be considered to be an excess of nuclear kinetic energy in S_1 after relaxation.

TABLE 2: Vertical Excitation Spectrum of Colchicina Arising from the $S_1 \rightarrow S_n$ Transition by Multireference CI at the Equilibrium Geometry of S_1[a]

n	assignment[b]	ΔE (eV)	f[c]
2	$5\pi \rightarrow 7\pi$	0.26	0.002
3	$n\mathrm{O} \rightarrow 6\pi$	0.41	0.000
4	$n\mathrm{O} \rightarrow 7\pi$	0.87	0.000
5	$6\pi' \rightarrow 6\pi$	1.13	0.024
6	ring to ring[d]	1.36	0.002
7	$5\pi 5\pi \rightarrow 6\pi 6\pi$	1.81	0.023
8	$6\pi' \rightarrow 6\pi$	2.19	0.011
9	ring to ring[d]	2.47	0.002
10	$5\pi 5\pi \rightarrow 6\pi 7\pi$ mixed	2.51	0.039
11	$4\pi 5\pi \rightarrow 6\pi 7\pi$	2.80	0.041
12	$4\pi \rightarrow 7\pi$	2.97	0.001

[a] The vertical transition $S_0 \rightarrow S_1$ is found at 4.08 eV and assigned to $5\pi \rightarrow 6\pi$. [b] Excitation label with respect to the main configuration of S_0. The normal labels indicate the molecular orbitals on the seven-atom ring. The prime is used for those localized on the trimethoxybenzene. The π orbitals on the two aromatic rings of colchicine are enumerated separately. The $6\pi'$ is the highest occupied orbital localized on trimethoxybenzene. [c] Oscillator strengths calculated in the mixed length−velocity gauge. [d] Mixing of $\pi \rightarrow \pi'$ and $\pi' \rightarrow \pi$ excitations with some contributions from double excitations.

To obtain the $S_1 \rightarrow S_n$ spectrum up to about 3 eV, a set of 14 states has to be considered in the multireference CI calculation. In this case, the inclusion of multiexcited detors is even more important in order to obtain reliable results. Indeed, whereas the first excited states are essentially single excitations with respect to S_0, some higher states are clearly recognized as double excitations. Therefore, the standard CIS method can be used for the geometry optimization of S_1, but more sophisticated techniques are to be used for the calculation of the S_1 absorption spectrum.

The excitation spectrum of S_1 is reported in Table 2. Because of the open-shell nature of all of the excited states considered in Table 2, it is probable that the energy errors due to the incomplete treatment of the electronic correlation are distributed in a more balanced way between the excited states.

As expected, the most intense transitions involve states with large components on detors that are single excitations with respect to S_1. In view of the absorption around 420 nm (2.95 eV) observed in the transient spectrum in Figure 4, S_{11} appears to be the most probable state responsible for such transitions. Indeed, the $S_1 \rightarrow S_{11}$ is the most intense excitation and agrees well with the observed excitation energy. As reported in Table 2, its main component is a double excited configuration with respect to S_0, corresponding in this case to a single excited configuration with respect to S_1.

On the basis of the above-reported data, we can formulate the conclusions of this work. Under the experimental conditions,

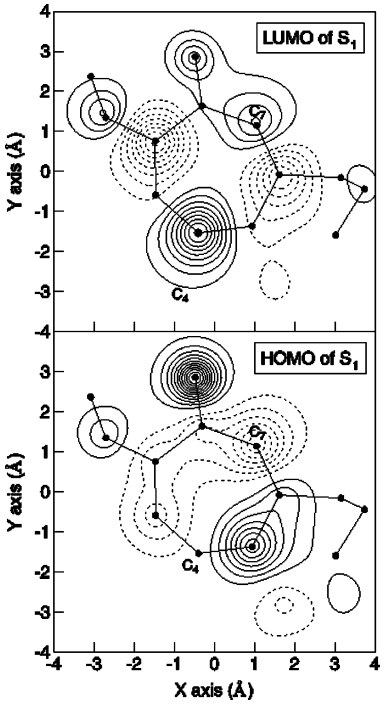

Figure 5. Contour map of the HOMO and LUMO for the first singlet excited state of colchicine in a plane parallel to the seven-ring plane. The distance between the planes is 0.6 Å.

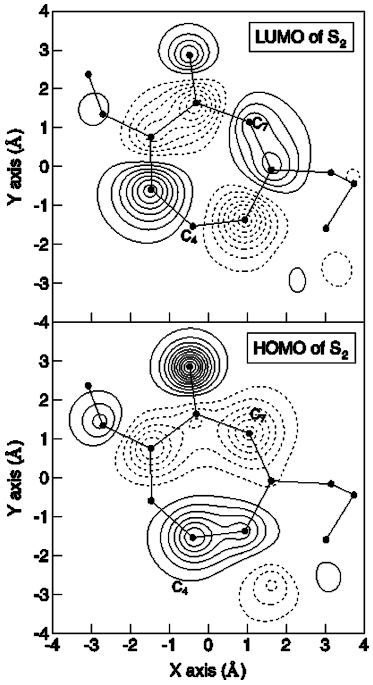

Figure 6. Contour map of the HOMO and LUMO for the second singlet excited state of colchicine in a plane parallel to the seven-ring plane. The distance between the planes is 0.6 Å.

the first singlet states of the two molecules are directly excited by the pump pulses. The small amount of extra energy with respect to the 0−0 transition is rapidly spread into the vibrational manifold of the S_1 state. In the case of colchicine, a rapid rearrangement of the structure with respect to that of the ground state follows, and we can observe a band that moves in less than 1 ps to shorter wavelengths. The lack of observation of an isosbestic point can be due to the concomitant presence of a vibrational cooling process and to an incomplete recovery of the white continuum dispersion. After that, a decay of the excited state follows. On the contrary, the biexponential decay observed in thiocolchicine can be due to the presence in the same spectral region of two states decaying with parallel and independent processes: (1) a direct decay to the ground state via a nonradiative pathway and (2) an ISC, which leads to a short-lived (<1 ns) triplet state. Such an assumption is consistent with the observation that often the $S_1 \rightarrow S_n$ and $T_1 \rightarrow T_n$ transitions fall in the same spectral region. Only the exact determination of the peak positions can help in disentangling the two contributions. This is not the case because we observe only the tail of the absorptions.

In our experience, an *f* value on the order of 0.01 corresponds to a strong transition, at least in the excited state. Although there is almost a factor of 10 difference with respect to the calculated value, we can safely attribute this spectral feature observed at 420 nm (2.95 eV) to the $S_1 \rightarrow S_{11}$ transition.

The fact that S_1 is populated by the pump beam and that no other bands show up after its decay leads us to suppose that the photocyclization of colchicines starts from this state. These results are in perfect agreement with those obtained in colchicone.[25]

Our observation is also in agreement with previous results, indicating that the photochemical conversion of colchicine to lumicolchicines does not involve or only partially involves triplet transients.

To ascertain the possibility that excited states S_1 and S_2 are consistent with the photochemical reaction affording lumicolchicines, we analyze their electronic distribution from the CI one-electron density matrix. The pertinent natural orbitals (those corresponding to an occupation number close to the unity) of the S_1 and S_2 states are reported in Figures 5 and 6, respectively. In Figure 5, it appears that the first singly occupied orbital, roughly corresponding to the HOMO in S_0, has nonbonding character with respect to the C_4 and C_7 atoms, whereas the second one, corresponding to the LUMO in S_0, can transform into a bonding $\sigma(C_4-C_7)$ by a disrotatory process. On the contrary, in the S_2 state (Figure 6) the two singly occupied orbitals are, respectively, antibonding and nonbonding for the C_4-C_7 pair. In this case, a disrotatory process would lead to an antibonding σ^* orbital, which does not seem to be consistent with the formation of stable photoproducts with one more σ bond.

The behavior of thiocolchicine is slightly different. First, we observe that after excitation a band appears and disappears with a time constant of 0.5 ps. The band is far into the red, but the remaining spectral features are approximately in the same region as those observed in the transients of colchicine. The band in the red can be attributed to an unrelaxed $S_1 \rightarrow S_n$ transition or to an $S_2 \rightarrow S_m$ transition. As previously mentioned, the band in the blue could be due to a triplet transition partially overlapping the $S_1 \rightarrow S_n$ transitions. In fact, such a large shift cannot be explained only in terms of rearrangement, as in the case of colchicine. This could explain why in the case of thiocolchicine the reactive pathway is quenched.

Acknowledgment. This work was supported by the Italian Ministero dell'Istruzione, dell'Università e della Ricerca (MIUR) and by the European Community under contract HPRI-CT1999-00111.

References and Notes

(1) Capraro, H. G.; Brossi, A. In *The Alkaloids*; Brossi, A., Ed.; Academic Press: New York, 1984; Vol. 23, pp 1−70.

(2) Boyè, O.; Brossi, A. In *The Alkaloids*; Brossi, A., Cordell, G. A., Eds.; Academic Press: New York, 1992; Vol. 4, pp 125−176.

(3) Weiner, J. L.; Buhler. A. V.; Whatlry, V. J.; Harris, R. A.; Dunwidie, T. V. *J. Pharmacol. Exp. Ther.* **1998**, *284*, 95−102.
(4) Staretz, M. E.; Hastie, S. B. *J. Org. Chem.* **1993**, *58*, 1589−1592.
(5) Helms, J. B.; Huang, L.; Price, R.; Sullivan, B. P.; Sullivan, B. A. *Inorg. Chem.* **1995**, *34*, 5335−5340.
(6) Berg, U.; Bladh, H.; Hoff, M.; Svensson, C. *J. Chem. Soc., Perkin Trans. 2* **1997**, 1697−1704.
(7) Grewe, R.; Wulf, W. *Chem. Ber.* **1951**, *84*, 621−625.
(8) Forbes, E. J. *J. Chem. Soc.***1955**, 3864−3870.
(9) Gardner, P. D.; Brandon, R. L. Haynes, G. R. *J. Am. Chem. Soc.* **1957**, *79*, 6334−6337.
(10) Chapman, O. L.; Smith, H. G.; King, R. W. *J. Am. Chem. Soc.* **1963**, *85*, 803−812.
(11) Pijsewska, L.; Kaul, J. L.; Joshi, R. K.; Santavy, F. *Collect. Czech. Chem. Commun.* **1967**, *32*, 158−170.
(12) Potesilova, H.; Alcaraz, C.; Santavy, F. *Collect. Czech. Chem. Commun.* **1969**, *34*, 2128−2133.
(13) Potesilova, H.; Wiedermannova, J.; Santavy, F. *Collect. Czech. Chem. Commun.* **1969**, *34*, 3642−3645.
(14) Canonica, L.; Danieli, B.; Manritto, P.; Russo, G. *Tetrahedron Lett.* **1969**, 607−608.
(15) Santavy, F.; Sedmera, P.; Snatzke, G.; Reichstein, J. *Helv. Chim. Acta* **1971**, *54*, 1084−1095.
(16) Takur, R. S.; Potesilova, H.; Santavy, F. *Planta Med.* **1975**, *28*, 201−209.
(17) Merchant, J. R.; Joshi, V. *Indian J. Chem., Sect. B* **1976**, *14*, 908−911.
(18) Malichova, V.; Potesilova, H.; Preininger, V.; Santavy, F. *Planta Med.* **1979**, *36*, 119−127.
(19) Gasic, O.; Popovic, M. *Herba Hung.* **1981**, *41*, 51−54.
(20) Sutlupinar, N.; Husek, A.; Potesilova, H.; Dvorackova, S.; Hanus, V.; Sedmera P.; Simanek, V. *Planta Med.* **1988**, *54*, 243−245.
(21) Husek, A.; Sutlupinar, N.; Sedmera, P.; Voegelein, F.; Valka, I.; Simanek, V. *Phytochemistry* **1990**, *29*, 3058−3060.
(22) Mihic, S. J.; Whatley, V. J.; Mcquilkin, S. J.; Harris, R. A. *J. Neurochem.* **1994**, *62*, 1790−1794.
(23) Roigt, H.; Leblanc, M. *Can. J. Chem.* **1973**, *51*, 2821−2827.
(24) Croteau, R.; Leblanc, R. *Photochem. Photobiol.* **1978**, *28*, 33−38.
(25) Bussotti, L.; D'Auria, M.; Foggi, P.; Lesma, G.; Righini, R.; Silvani, A. *Photochem. Photobiol.* **2000**, *71*, 29−34.
(26) Nery, A. L. P.; Quina, F. H.; Moreira, P. F.; Medeiros, C. E. R.; Baader, W. J.; Shimizu, K.; Catalani, L. H.; Bechara, E. J. H. *Photochem. Photobiol.* **2001**, *73*, 213−218.
(27) Neuwhal, F. V. R.; Bussotti, L.; Foggi, P. In *Res. Adv. Photochem. Photobiol.* **2000**, *1*, 77−94.
(28) Bussotti, L.; Foggi, P.; Gellini, C.; Moroni, L.; Salvi, P. R. *Phys. Chem. Chem. Phys.* **2001**, *3*, 3027−3033.
(29) Foggi, P.; Bussotti, L.; Neuwahl, F. V. R. *Int. J. Photoenergy* **2001**, 3, 103−109.
(30) Becke, A. D. *J. Chem. Phys.* **1996**, *98*, 5648−5652.
(31) Frisch, M. J.; Trucks, G. W.; Schlegel, H. B.; Scuseria, G. E.; Robb, M. A.; Cheeseman, J. R.; Zakrzewski, V. G.; Montgomery, J. A., Jr.; Stratmann, R. E.; Burant, J. C.; Dapprich, S.; Millam, J. M.; Daniels, A. D.; Kudin, K. N.; Strain, M. C.; Farkas, O.; Tomasi, J.; Barone, V.; Cossi, M.; Cammi, R.; Mennucci, B.; Pomelli, C.; Adamo, C.; Clifford, S.; Ochterski, J.; Petersson, G. A.; Ayala, P. Y.; Cui, Q.; Morokuma, K.; Malick, D. K.; Rabuck, A. D.; Raghavachari, K.; Foresman, J. B.; Cioslowski, J.; Ortiz, J. V.; Stefanov, B. B.; Liu, G.; Liashenko, A.; Piskorz, P.; Komaromi, I.; Gomperts, R.; Martin, R. L.; Fox, D. J.; Keith, T.; Al-Laham, M. A.; Peng, C. Y.; Nanayakkara, A.; Gonzalez, C.; Challacombe, M.; Gill, P. M. W.; Johnson, B. G.; Chen, W.; Wong, M. W.; Andres, J. L.; Head-Gordon, M.; Replogle, E. S.; Pople, J. A. *Gaussian 98*, revision A.1; Gaussian, Inc.: Pittsburgh, PA, 1998.
(32) Huron, B.; Malrieu, J. P.; Rancurel, P. *J. Chem. Phys.* **1973**, *58*, 5745−5759.
(33) Angeli, C.; Persico, M. *Theor. Chem. Acc.* **1997**, *98*, 117−128.
(34) Cimiraglia, R. *J. Chem. Phys.* **1985**, *83*, 1746−1749.